Turbophoresis attenuation in a turbulent channel flow with polymer additives

Arash Nowbahar[1], Gaetano Sardina[2,3]†,
Francesco Picano[3], and Luca Brandt[3]

[1]Department of Chemical Engineering, The Grove School of Engineering, The City College of New York, CUNY, NY 10031, USA

[2] Facoltà di Ingegneria, Architettura e Scienze Motorie, UKE Università Kore di Enna, 94100 Enna, Italy

[3]SeRC (Swedish e-Science Research Centre) and Linné FLOW Centre, KTH Mechanics, SE-100 44 Stockholm, Sweden

Turbophoresis occurs in wall-bounded turbulent flows where induces a preferential accumulation of inertial particles towards the wall and is related to the spatial gradients of the turbulent velocity fluctuations. In this work, we address the effects of drag reducing polymer additives on turbophoresis in a channel flow. The analysis is based on data from a direct numerical simulation (DNS) of the turbulent flow of a viscoelastic fluid modeled with the FENE-P closure and laden with particles of different inertia. We show that polymer additives decrease the particle preferential wall accumulation and demonstrate with an analytical model that the turbophoretic drift is reduced because the wall-normal variation of the wall-normal fluid velocity fluctuations decreases. As this is a typical feature of drag reduction in turbulent flows, an attenuation of turbophoresis and a corresponding increase in the particle streamwise flux are expected to be observed in all these flows, e.g. fiber or bubble suspensions and MHD.

Key words:

1. Introduction

The near-wall accumulation of inertial particles, i.e. turbophoresis, in wall-bounded, turbulent flows is an important phenomenon when describing systems with particle-fluid-wall interactions. Turbophoresis can lead to particle concentrations at the wall up to hundred times the bulk value, (e.g. Soldati & Marchioli 2009; Sardina *et al.* 2012*a*). Examples where turbophoresis may play a role include reactors, filters, aircraft engines and turbines, e.g. Grindle *et al.* (2003). In such systems particle accumulation may negatively or positively affect the system efficiency. Turbophoresis has been characterized in many studies, one of the first being that by Caporaloni *et al.* (1975). The theoretical analysis by Reeks (1983) showed the relation between the net particle flux and the particle velocity skewness. Since then, numerous papers have studied the accumulation of inertial particles in various geometries, using theoretical approaches (Young & Leeming 1997; Zaichik 1999), experimental (Liu & Agarwal 1974; Wu & Young 2012) and computational techniques (Rouson & Eaton 2001; Marchioli *et al.* 2008; Sardina *et al.* 2012*b*). It has been shown that a bias in following sweep and ejection events, which characterize

† Email address for correspondence: gaetano@mech.kth.se

wall-turbulence, lead to a net particle transfer towards the wall. A strong correlation is found between accumulation and coherent near-wall structures that force the particles to remain in regions of slow moving fluid, i.e. low speed streaks (see Soldati & Marchioli 2009, for a review). Considering particles much denser than the fluid, the main parameter describing their inertial properties is the relaxation, or Stokes, time $\tau_p = \rho_p d_p^2/(18\rho\nu)$, where ρ and ρ_p are the fluid and particle densities, d_p the particle diameter, and ν the fluid kinematic viscosity. Small τ_p represent particles that behave almost as fluid tracers, while large relaxation times correspond to particles that are unaffected by turbulent fluctuations. Turbophoresis is maximum when τ_p is of the order of the characteristic time of the near-wall coherent structures (buffer layer), corresponding to about 20 viscous time scales ν/u_τ with $u_\tau = \sqrt{\tau_w/\rho}$ the friction velocity and τ_w the stress at the wall (Soldati & Marchioli 2009). Large part of the studies mentioned above have considered particles with density larger than that of the carrier phase and dilute conditions thus neglecting particle momentum transfer towards the fluid and mutual particle interactions (one-way coupling).

Whereas turbophoresis is characteristic of wall-bounded flows, small-scale clustering is observed for both homogeneous and wall-bounded flow, e.g. Wang & Maxey (1993). Small-scale clustering appears as high local concentrations of particles and corresponding void regions, meaning a loss in spatial homogeneity of the particle distribution. This phenomenon is attributed to particle inertia that, selectively filtering turbulent fluctuations, prevents particles from following highly convoluted trajectories. Clustering is maximum when τ_p is of the order of the Kolmogorov dissipative time scale; it is therefore controlled by small-scale turbulence (Bec *et al.* 2007). In wall turbulence, the small-scale clustering and turbophoresis phenomena are entangled since particles preferentially accumulate in regions of fluid motions directed away from the wall. This balances the turbophoretic drift towards the wall and the system reaches steady state conditions as shown in Picano *et al.* (2009); Sardina *et al.* (2012*a*).

Thus far most studies of inertial particles involve the use of Newtonian fluids; however polymer solutions are of definitive interest also due their commercial and industrial relevance (Sellin *et al.* 1982). In particular, particle-laden fluids with polymer additives are important in industrial process related to coatings, paints, inks and polymeric adhesives. All these fluids are constituted by a polymeric solution to which a specific metallic powder is added to obtain the desired chromatic or thermo-chemical features, see e.g. Visconti *et al.* (2001); Urban & Takamura (2002); Vogler *et al.* (2010). The addition of polymers to Newtonian fluids presents interesting properties such as drag reduction (Virk 1975). Though a precise description of the drag reduction mechanism is still lacking, it is known that polymer additives deeply change the coherent structures of the near-wall region leading to an increase of the streamwise velocity fluctuation and a reduction of the cross-stream components (De Angelis *et al.* 2002; Xi & Graham 2010). The strong alteration of the wall turbulence is expected to affect also the particle transport.

In a recent paper, De Lillo, Boffetta & Musacchio (2012) investigate the effects of polymer additives on small-scale clustering of heavy and light inertial particles in homogeneous isotropic turbulence. They find that depending on particle and flow parameters (namely the particle relaxation time and the polymer relaxation time), polymers can either increase or decrease clustering. The aim of the present work is to study for the first time the effects of polymer additives on turbophoresis. This issue is addressed by analyzing data of a DNS of a particle-laden turbulent channel flow at a friction Reynolds number $Re_\tau = u_\tau h/\nu = 150$. The Eulerian flow solver uses the FENE-P model to account for the effects of the polymer solution, while a Lagrangian solver is used to track the position and velocity of particle populations with different τ_p. In contrast to the case

of small-scale clustering, the results show that the wall particle concentration is always lowered by the presence of polymer additives, i.e. turbophoresis is reduced. We show that this attenuation is linked to the reduction of the wall-normal derivative of the magnitude of the wall-normal velocity fluctuations that is typical of all turbulent flows of reduced drag. Hence, we argue that the turbophoretic drift is lower in all turbulent flows when drag is reduced, e.g. fiber and bubble suspensions, MHD (see Lee & Duffy 1976; Tsinober 1990; Van Den Berg *et al.* 2005, among others). A simple predictive model is derived in the limit of small particle inertia to quantify the reduction of turbophoresis.

2. Methodology

A coupled Eulerian-Lagrangian numerical method has been used to perform the simulations of a particle-laden turbulent channel flow. To model the viscoelastic carrier phase, the Finitely-Extensible-Nonlinear-Elastic-Peterlin (FENE-P) approximation is used. This simple model has been shown to reproduce some of the important features of polymer additives such as drag reduction (Sureshkumar *et al.* 1997; De Angelis *et al.* 2002). In this model, the finite extensibility of the polymer is taken into account in a nonlinear fashion. The fluid velocity field $\mathbf{u}(\mathbf{x}, t)$ and the polymer conformation tensor $\boldsymbol{\sigma}(\mathbf{x}, t)$ are governed by the following dimensionless equations

$$\frac{\partial \mathbf{u}}{\partial t} + \mathbf{u} \cdot \nabla \mathbf{u} = -\nabla p + \frac{\beta}{Re} \nabla^2 \mathbf{u} + \frac{1 - \beta}{Re} \nabla \cdot \left(\frac{f\boldsymbol{\sigma} - \mathbf{I}}{Wi} \right) \tag{2.1}$$

$$\frac{\partial \boldsymbol{\sigma}}{\partial t} + \mathbf{u} \cdot \nabla \boldsymbol{\sigma} = (\nabla \mathbf{u})^T \cdot \boldsymbol{\sigma} + \boldsymbol{\sigma} \cdot \nabla \mathbf{u} - \frac{f\boldsymbol{\sigma} - \mathbf{I}}{Wi}. \tag{2.2}$$

f is the Peterlin function defined as $f = (L^2 - L_0^2)/(L^2 - \tilde{r}^2)$, where $\tilde{r}$ is the root mean square chain extension, L is the maximum chain extension, L_0 is the equilibrium length of the chains, p is pressure, I the identity tensor, and β is the ratio of the solvent viscosity to the total viscosity. The response time of the polymer, τ_{pol}, represents the longest relaxation time for a polymer chain to return to the equilibrium position. The relevant dimension-less parameter is the Weissenberg number, defined as the ratio of the polymer relaxation time τ_{pol} to a characteristic time of the flow, i.e. $Wi = \tau_{pol}/(h/U_c)$ with U_c the centerline velocity of the corresponding laminar case and h the channel half-width. This value measures the extent to which polymers are elongated by the flow. We performed simulations at two different Weissenberg numbers $Wi = 5, 10$; these can also be expressed in inner units by introducing the friction Weissenberg number $Wi_\tau = \tau_{pol} u_\tau^2/\nu = 31.25, 62.5$. For a polymer relaxation time smaller than the characteristic flow time scale the polymer tends to maintain its unperturbed equilibrium configuration, while in the opposite limit the polymer is always significantly elongated. In the former limit, a Newtonian viscous behavior is expected, while in the latter an elastic solid-like behavior (De Angelis *et al.* 2002). The second control parameter is the Reynolds number $Re = U_c h/\nu = 3600$. It is common in wall turbulence to adopt the friction Reynolds number $Re_\tau = u_\tau h/\nu$ that is here fixed at $Re_\tau = 150$. The factor β has been fixed at the value of 0.95 for both the viscoelastic simulations.

The DNS data in the channel-flow geometry are obtained with the pseudo-spectral Navier-Stokes solver SIMSON (Chevalier *et al.* 2007). For the fluid phase, streamwise and spanwise directions are discretized with Fourier series, whereas the wall-normal direction is expanded in Chebyshev polynomials. A low-storage three-stage mixed Runge-Kutta/Crank-Nicolson scheme is employed for temporal discretization. The numerical integration of the particles is achieved using a second order Adams-Bashforth method (Sardina *et al.* 2012a). The size of the computational domain used is $2\pi h \times 2h \times 2\pi h$

in the streamwise, wall-normal and spanwise directions, respectively, discretized with a total of $96 \times 97 \times 128$ spectral modes. The origin of the reference system is placed in the mid-plane of the channel with the x-axis oriented with the mean flow direction, the y-axis directed along the wall-normal direction and oriented towards the upper-wall and the z-axis in the spanwise direction according to the right-hand rule.

We assume a dilute suspension of particles made of rigid spheres whose diameter is smaller than the viscous scales of turbulence and the density is larger than that of the fluid. The only force acting on these particles is the viscous Stokes drag, hence we neglect particle feedback on the carrier phase, inter-particle collisions and mutually hydrodynamic coupling (Maxey & Riley 1983). The Lagrangian evolution of the particles is given by:

$$\frac{d\mathbf{v_p}}{dt} = \frac{\mathbf{u}(\mathbf{x_p}, t) - \mathbf{v_p}}{St}(1 + 0.15 Re_p^{0.687})\,\chi, \qquad (2.3)$$

$$\frac{d\mathbf{x_p}}{dt} = \mathbf{v_p}, \qquad (2.4)$$

where x_p and v_p are the position and velocity of the p$^{\text{th}}$ particle, $Re_p = |\mathbf{v_p} - \mathbf{u_p}| d_p / \nu$ is the particle Reynolds number (d_p particle diameter) and St is the dimensionless form of the particle relaxation time, $St = \tau_p/(h/U_c)$. The correction factor χ is introduced in the Stokes drag to account for the effects of a finite Weissemberg number at the particle size, $Wi_p = \tau_{pol} |v_p - u|/(d_p/2)$. Chhabra *et al.* (1980) found that the Stokes drag in a polymeric fluid matches the Newtonian value when $Wi_p \leqslant 0.1$ ($\chi = 1$) and it is reduced to $\chi = 0.74$ when $Wi_p \geqslant 0.66$. A sharp transition occurs between these asymptotic values in the intermediate range $0.1 \leqslant Wi_p \leqslant 0.66$. We reproduced this behavior exploiting for this intermediate range the expression $\chi = -0.14 \log(Wi_p) + 0.68$ that well fits the experimental data of Chhabra *et al.* (1980). We performed some preliminary simulations (not reported) neglecting the viscoelastic effects on the particle drag, $\chi = 1$, and assuming that the particle relaxation time is independent of the particle Weissenberg number Wi_p. No relevant differences emerge for the qualitative behavior described in the following, although small quantitative variations are observed in the range of Wi investigated. The present formulation is more general and correct and it can be fruitfully exploited in future studies covering a different parameter range.

It convenient to define also the Stokes number based on the inner flow units, $St^+ = \tau_p u_\tau^2 / \nu$ that is the only parameter varied in this work since the density ratio between the particle and fluid is kept at $\rho_p / \rho = 15$. The value of the density has been fixed considering liquids with polymeric additives filled with a metallic powder as often occur in paints, adhesives, glues and coatings to alter chromatic, thermo-electrical and mechanical properties, e.g. epoxy coating/adhesive ($\rho = 1,000 - 1,600 \, Kg/m^3$) with silver, tungsten and gold powders ($\rho_p = 10,000 - 19,000 \, Kg/m^3$), see e.g. Visconti *et al.* (2001); Urban & Takamura (2002); Vogler *et al.* (2010).

Four particle populations are considered $St^+ = 0, 1, 10, 20$ with a total of 1,000,000 particles per simulation; these values correspond to a physical situation where the particle relaxation time τ_p ranges from 0.0015 to 0.03 seconds while the particle diameter ranges from 130 μm to 600 μm if, for example, we assume a half-channel width $h = 2cm$. Periodic boundary conditions are considered in the streamwise and spanwise directions for the evolution of the particles. Particle collisions with walls (when particle positions are half the diameter away from the wall) are treated as purely elastic. The turbulent flow was initialized using a localized disturbance to promote the transition to turbulence. To gather flow statistics, we waited until the flow reached a statistical steady state, independent of the initial conditions, at $t^+ = 6000$. Only then, the particles are injected
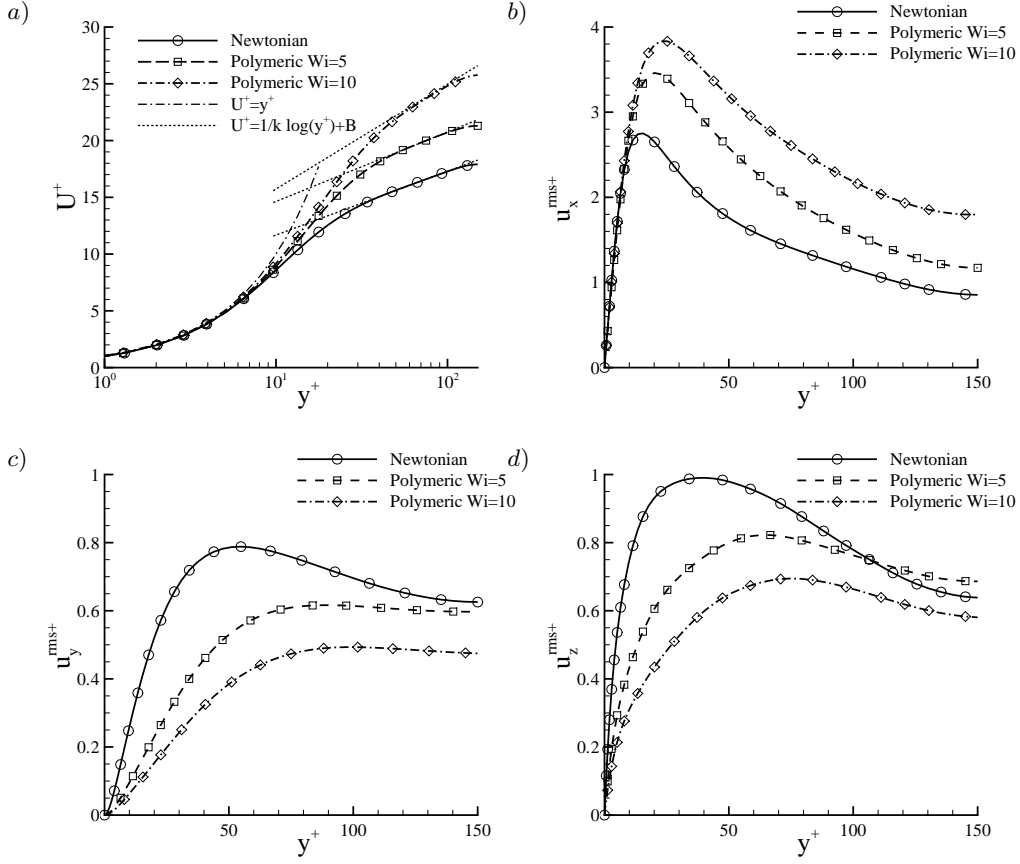
a)

FIGURE 1. *a*) Mean streamwise velocity (*a*) $U^+ = \langle u_x \rangle / u_\tau$ vs the wall normal direction y^+. The dash-dotted line denotes $U^+ = y^+$, the dotted lines the log fits $U^+ = 1/k \log(y^+) + B$ with $k = 0.41$ and $B = 6.1$ for the Newtonian case, $k = 0.38$ and $B = 8.5$ for the visco-elastic one with $Wi = 5$ and $k = 0.3$ and $B = 9.7$ for $Wi = 10$. Root-mean-square of velocity fluctuations: u_x^{rms}/u_τ streamwise (*b*), u_y^{rms}/u_τ wall-normal (*c*) and u_z^{rms}/u_τ spanwise component (*d*) vs the wall-normal direction y^+.

into the domain with a random distribution; the statistical steady state is reached by the particle phase at $t^+ = 30,000$ when we started to collect statistical independent samples (around 500) over a time interval of $t^+ = 30,000$.

To discern the effects of the polymer additives on particle transport, we perform a simulation of the Newtonian channel flow for the same pressure gradient, $Re_\tau = 150$, and particle populations. Data are collected after the system has reached the statistical steady state. More informations and details about the numerical implementation can be found in Sardina *et al.* (2012*a,b*) for Newtonian cases.

3. Results.

Figure 1*a*) shows the mean streamwise velocity $U^+ = \langle u_x \rangle / u_\tau$ profile across the wall normal direction $y^+ = (h - y)/(\nu/u_\tau)$ for both the polymeric and Newtonian carrier phases. While near the wall the velocity of the polymeric and Newtonian cases are similar, towards the center of the channel they deviate, with the polymeric cases showing
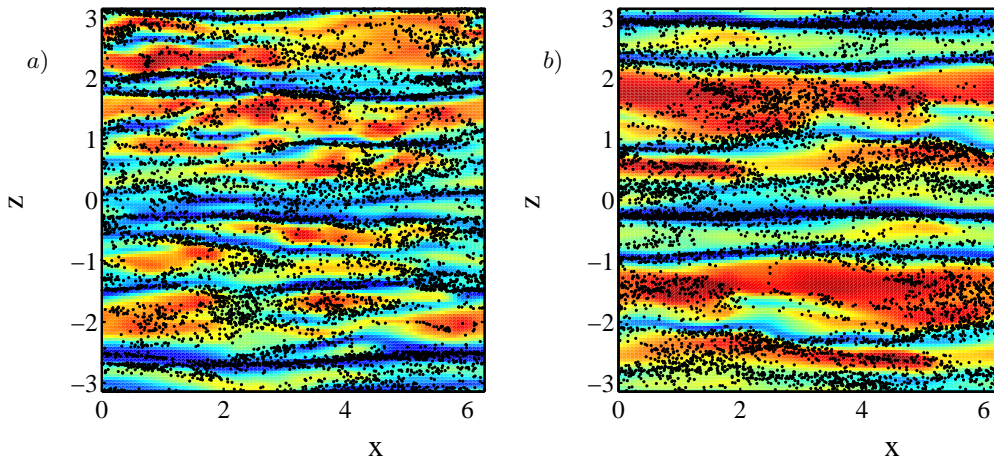
FIGURE 2. Snapshot of an $x - z$ plane in the buffer layer at $y^+ = 15$ for a) Newtonian case and b) polymeric flow at $Wi = 5$. Black dots represent particles in the slab $10 \leqslant y^+ \leqslant 20$, and colors indicate the magnitude of the stream-wise velocity component, red being highest and blue lowest.

larger values that increase with the Weissenberg number Wi. Given that all the cases are run with the same pressure gradient, i.e. u_τ, the increase in mean velocity indicates drag reduction with the addition of polymers as found in other studies, see e.g. Virk (1975); Sureshkumar *et al.* (1997). The profiles of the fluctuating velocity components are shown for Newtonian and polymeric flows in the figures $1b$), $1c$), $1d$). The plots show an increase of the root mean square (r.m.s.) streamwise velocity fluctuation u_x^{rms}/u_τ (b) with the addition of polymers, but decreasing wall-normal u_y^{rms}/u_τ (c) and spanwise u_z^{rms}/u_τ (d) r.m.s. velocity fluctuations. The effect is more intense at the higher Weissenberg number. These trends are consistent with available literature for channel flow with polymer additives (e.g. De Angelis *et al.* 2002) and are common also to other drag reducing flows (Virk 1975; Lee & Duffy 1976; Tsinober 1990; De Angelis *et al.* 2004; Van Den Berg *et al.* 2005).

Figure 2 shows instantaneous snapshots of a wall-parallel plane in the buffer region ($5 < y^+ < 30$). The contours represent the streamwise fluctuation u_x' of the carrier fluid velocity at the location $y^+ = 15$ where there is the peak of the turbulent kinetic energy for the Newtonian flow, red being high and blue the low-speed fluid. Black dots represent the particles around that plane ($y^+ = [10 \div 20]$) and the snapshot is taken at statistical steady state. For the Newtonian case (a), we see streaks of low and high speed fluid, as well as streaks of particles aligning preferentially in the regions of low-speed fluid. This phenomenon is well documented in several works, e.g. Soldati & Marchioli (2009), and is a characteristic of fully developed statistically steady states, Picano *et al.* (2009). In these conditions, when the mean particle concentration profile does not change any more, the turbophoretic drift is balanced by the oversampling of the fluid motions departing from the wall, those associated to the low-speed streaks. Hence, particles are found to preferentially accumulate in elongated structures localized in the low fluid-velocity streaks at statistical steady state.

Figure 2b) shows a similar snapshot for the viscoelastic flow at $Wi = 5$. It is confirmed that polymers tend to widen the streaks occurring in the velocity field (De Angelis *et al.* 2002). The effects of polymers on the flow are mostly seen in the buffer layer, where they increase the fluids resistance to extensional deformation, making eddies wider and

less frequent. In this flow, inertial particles, like in Newtonian flow, align into streaks; however we see a decreased tendency to preferentially localize in low-speed regions. With the widening of these streaks, the particles appear to experience less clustering: they are spread out more than in the Newtonian case. This phenomenology will be quantitatively characterized in the following analyzing the probability density functions (p.d.f.) of the fluid velocities sampled by particles for the Newtonian and viscoelastic cases and comparing the data with the unconditioned fluid velocity p.d.f.s.

The turbophoretic drift induces a mean particle migration towards the wall that is quantified by the mean particle concentration c/c_0, defined as the ratio of the time-averaged particle number per unit volume normalized by the bulk concentration. Figure 3 shows the concentration profile c/c_0 against the wall normal direction y^+. For the Newtonian and polymer flows we observe high concentrations of particles at the wall (turbophoresis) as compared to the bulk. For $St^+ = 1$ (a), the particles are dispersed throughout the channel with only slight accumulation at the wall. Most interestingly, the addition of polymers leads to a decrease in concentration in the near-wall region, which correspond to higher concentrations in the bulk, for all Stokes number investigated. Larger the Weissenberg number Wi, more accentuated is the effect. The decrease in the wall concentration for the polymeric flows is most pronounced for $St^+ = 10$ (b), where the concentration decreases by more than two times for $Wi = 5$ and more than five times for $Wi = 10$.

As the particle wall-accumulation is linked to the particle preferential sampling of slow fluid and ejection events, we report the probability density functions (p.d.f.) of the fluid velocity sampled by particles in figure 4 for the Conian and polymeric flows and different particle populations in the steady state regime. We assume that positive values of the fluid velocity sampled by the particles indicate velocity directed towards the walls. Considering first the Newtonian case, panel a), it is apparent that accumulating particles ($St^+ = 10, 20$) tend to avoid intense fluid motions directed towards the wall, $u_y'^+ > 0$, showing values lower than the fluid on the positive side of the p.d.f.. The particles tend to oversample the slow departing motions, small negative values, as displayed in the inset of the figure. The situation drastically changes for the viscoelastic cases, panels b) and c) of figure 4. The preferential sampling of the slow departing motions is not evident anymore expecially for the case $Wi = 10$, although also in these cases the particles with $St^+ = 10, 20$ tend to filter strong approaching fluid motions. The qualitative behavior observed in the istantaneous snapshots of figure 2 is here quantitatively characterized by the p.d.f of the fluid velocity. Particles in the Newtonian fluid oversample slow fluid motions departing from the wall towards the channel center because of the preferential localization in the low-speed streaks. In viscoelastic fluid this phenomenon appears to be strongly attenuated. We recall that in wall turbulence the low-speed streaks are characterized by a lower streamwise velocity fluctuation and slow outward fluid motions (ejection events), in contrast the high-speed streaks are associated with high streamwise velocity fluctuations together with fast inward fluid motions (sweep events).

In order to show the link between preferential sampling and accumulation, explaining in this way the reduced particle accumulation observed at the wall in the turbulent channel flow with polymer additives, it is useful to work under the assumption of small particle relaxation times τ_p. Under this hypothesis, we can safely consider vanishing particle Reynolds and Weissenberg numbers and simplify the particle dynamics equation (2.3) to

$$\mathbf{u}(\mathbf{x_p}, t) = \mathbf{v_p} + St \frac{d\mathbf{v_p}}{dt}. \qquad (3.1)$$
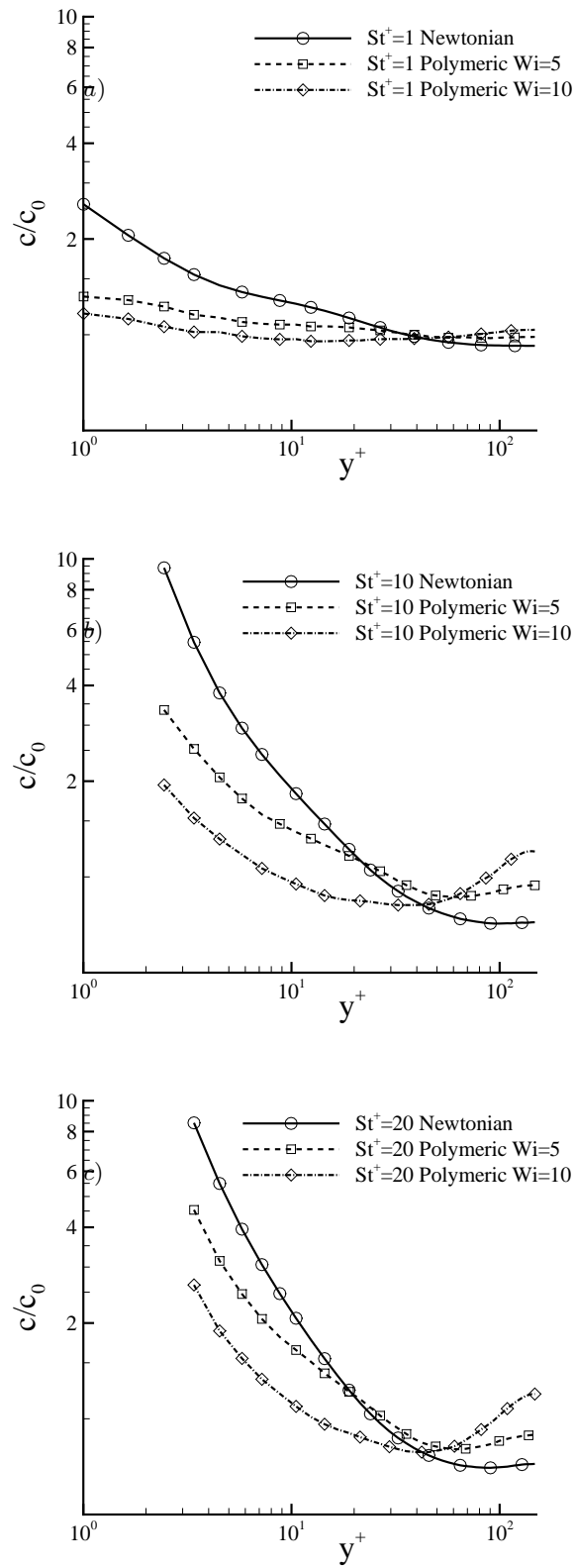
FIGURE 3. Mean particle concentration c/c_0 as a function of y^+ for different Stokes numbers $St^+ = 1$ (a), $St^+ = 10$ (b), $St^+ = 20$ (c).

Taking the time derivative of the flow velocity following the particle trajectory (Picano *et al.* 2011), we obtain:

$$\frac{d\mathbf{u}(\mathbf{x_p}, t)}{dt} = \frac{d\mathbf{v_p}}{dt} + St\frac{d^2\mathbf{v_p}}{dt^2} \tag{3.2}$$

$$\frac{\partial\mathbf{u}(\mathbf{x_p}, t)}{\partial t} + \mathbf{v_p} \cdot \nabla\mathbf{u}(\mathbf{x_p}, t) = \frac{d\mathbf{v_p}}{dt} + St\frac{d^2\mathbf{v_p}}{dt^2} \tag{3.3}$$

where indicating with $D/Dt = \partial/\partial t + \mathbf{u} \cdot \nabla$ the material derivative following the fluid trajectory we can re-write the last equation as:

$$\frac{d\mathbf{v_p}}{dt} = \left.\frac{D\mathbf{u}}{Dt}\right|_{x=x_p} - (\mathbf{u} - \mathbf{v_p}) \cdot \nabla\mathbf{u} - St\frac{d^2\mathbf{v_p}}{dt^2}. \tag{3.4}$$

Substituting this last expression in (3.1) and considering that $\mathbf{u} - \mathbf{v_p} = St\,d\mathbf{v_p}/dt$, we obtain an estimate of the particle velocity for small Stokes numbers,

$$\mathbf{v_p} = \mathbf{u}(\mathbf{x_p}, t) - St\,\left.\frac{D\mathbf{u}}{Dt}\right|_{x=x_p} + \mathcal{O}(St^2) \tag{3.5}$$

that can be conveniently expressed in viscous units neglecting second order corrections as

$$\mathbf{v_p^+} \simeq \mathbf{u^+}(\mathbf{x_p}, t) - St^+\,\mathbf{a_{f|x=x_p}^+}. \tag{3.6}$$

Taking the average of equation (3.6) and projecting onto the wall-normal direction

$$\langle v_{p_y}^+ \rangle = \langle u_y|_p^+ \rangle + St^+ \frac{d\langle u_y'^{2+} \rangle}{dy^+}, \tag{3.7}$$

where it should be noted that according to our convention $y^+ = (h-y)u_\tau/\nu$ and velocities towards the walls are positive. From equation (3.7), the mean wall-normal particle velocity is equal to the sum of the mean wall-normal fluid velocity sampled by the particles and the turbophoretic drift $TD^+ = St^+ d\langle u_y'^{2+} \rangle/dy^+$ (Reeks 1983). At the earlier stages when particles are still evenly distributed and $\langle u_y|_p^+ \rangle = 0$, particles start to accumulate at the wall because the turbophoretic drift is directed towards the wall, $TD^+ > 0$, i.e. $\langle v_{p_y}^+ \rangle = TD^+ > 0$. After some time, at statistical steady conditions, the mean particle wall-normal velocity, $\langle v_{p_y}^+ \rangle = 0$. This implies that particles have to oversample fluid departing events ($u_y^+ < 0$), so that $\langle u_y|_p^+ \rangle = -TD^+$. As a consequence the particles tend to concentrate preferentially in the low-speed streaks where the wall-normal fluid velocity is directed away from the wall, as discussed above.

The model applies both to the Newtonian and to the polymeric cases and it should be noted that, fixed St^+, the turbophoretic drift TD^+ is controlled only by the wall-normal derivative of the normal stress $\langle u_y'^{2+} \rangle$. As it can be appreciated from figure 1, the derivative of the wall-normal normal stress in the buffer layer is much smaller in the polymeric flows than in the Newtonian one. Hence inertial particles in wall-bounded flows with polymer additives are subjected to a smaller turbophoretic drift that is the cause of a reduced wall accumulation. This connection with the gradients of the wall-normal velocity fluctuations is more general and can be applied to understand flows of different Reynolds numbers or in different configurations.

The equation (3.7) also explains why the particles are much less correlated with the low-speed streaks in the polymeric flows where the turbophoretic drift, balanced by the
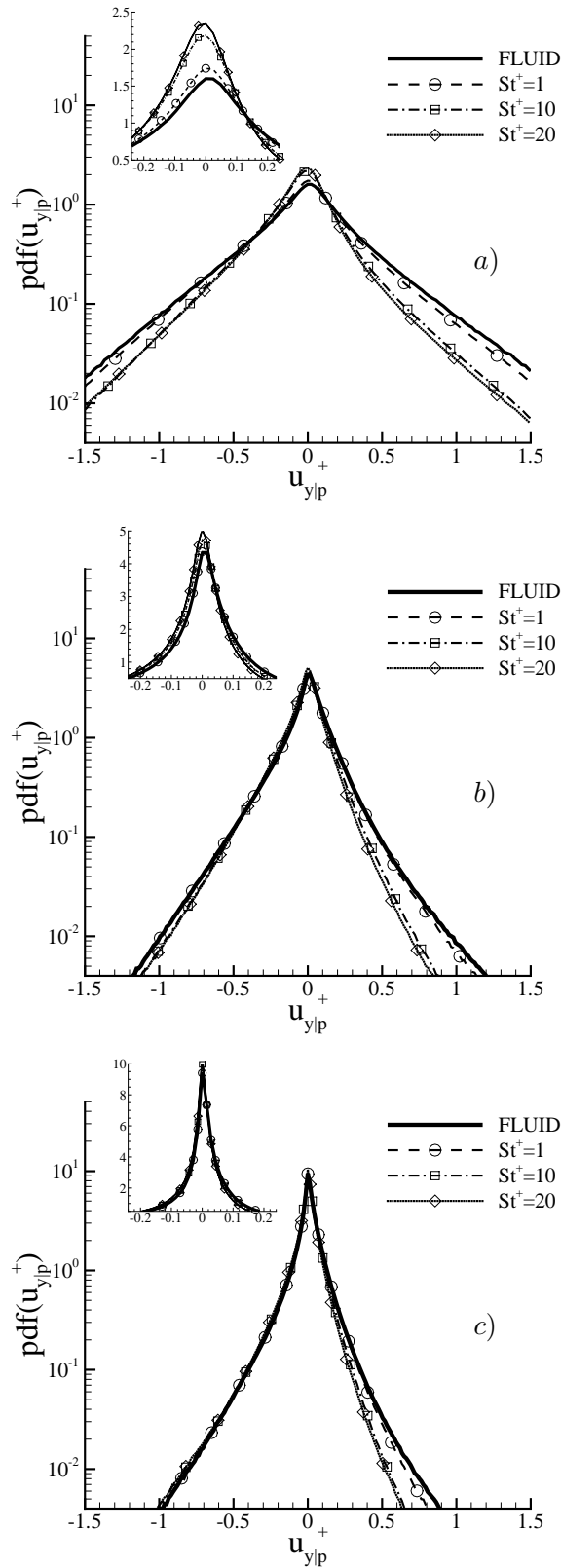
FIGURE 4. The p.d.f.s of wall-normal fluid velocity sampled by particles for a) the Newtonian, b) the polymeric flow with $Wi = 5$ and c) the polymeric flow with $Wi = 10$ in the buffer layer at statistically steady state. Positive wall-normal velocities are directed towards the wall. Enlargement of the slow velocity events are provided in the insets.
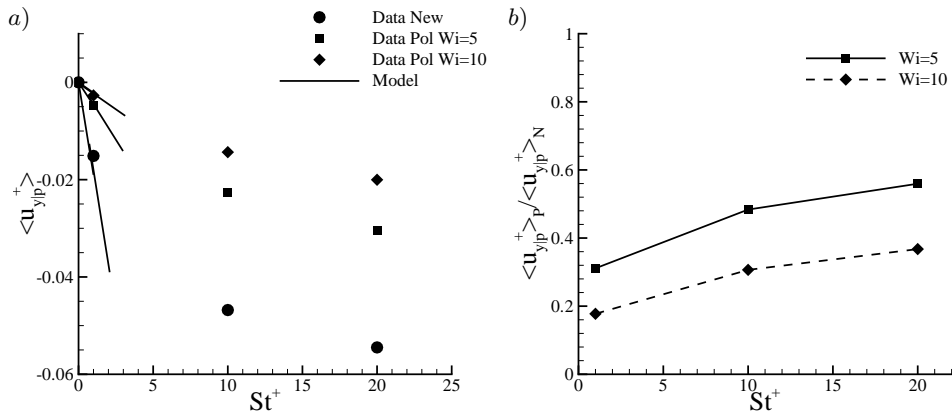
FIGURE 5. *a*) Mean wall-normal fluid velocity sampled by particles $\langle u_y|_p^+ \rangle$ vs Stokes number St^+ for polymeric and Newtonian cases. *b*) Ratio between $\langle u_y|_p^+ \rangle$ in the polymeric and Newtonian flows as a function of St^+.

preferential sampling of the fluid departing velocities, is lower. Figure 5*a*) shows the mean fluid velocity sampled by the particles (symbols) together with the estimate for this quantity provided by the wall-normal derivative of the normal stress $\langle u_y'^{2+} \rangle$ (solid lines for $St^+ < 3$). In fully developed conditions, the turbophoretic drift coincides with mean fluid velocity sampled by the particles, $\langle u_y|_p^+ \rangle = -TD^+$, and is negative, meaning drift towards the wall. The lines properly match the numerical data for small Stokes numbers, $St^+ = \mathcal{O}(1)$, where the particle acceleration is well approximated by the fluid acceleration. The model predicts a linear behavior with St^+ with a decreased slope for the viscoelastic cases: The turbophoretic drift is reduced (about one third at $Wi = 5$ and one fifth at $Wi = 10$) by the presence of polymer additives. Increasing the Stokes number, the turbophoretic drift still increases with St^+, though not linearly. Nonetheless we find a similar attenuation of the turbophoretic drift for the viscoelastic cases also for particles with stronger inertia, see figure 5*b*). Even though the assumptions of the proposed model, eq. (3.7), are not verified for large St^+, the observed behavior is qualitatively the same.

4. Final Remarks.

DNS of a turbulent channel flow at $Re_\tau = 150$ laden with inertial particles are performed with both Newtonian and polymeric fluid. For all cases investigated, we observe large concentrations of particles near the wall, i.e. turbophoresis, and particle clustering into streaks in the buffer layer, but with different intensities.

The significant finding of our work concerns the effects of drag reducing polymers on the turbophoresis. We find that with the addition of polymers there is a reduction of the particle accumulation at the wall with respect the Newtonian turbulent flow driven by the same pressure gradient (Re_τ). The attenuation is more intense when increasing the Weissenberg number. The polymers alter the structure of the turbulent flow: they decrease small-scale turbulence, elongate and widen velocity streaks in the buffer layer resulting in a reduction of the fluid velocity wall-normal fluctuations. The attenuation of $\langle u_y'^{2+} \rangle$ near the wall is coupled with a reduction of its wall-normal derivative that controls the turbophoretic drift. The reduced drift is the cause of the decrease of the turbophoresis, i.e. of the particle wall concentration. The modification of the carrier flow in the buffer layer, caused by polymers, decreases also the clustering of particles which

preferentially localize into the low-speed streaks in the Newtonian case. Hence, polymers alter the delicate balance that leads to a fully developed (steady state) accumulation at the wall, by decreasing the turbophoretic drift and affecting the preferential sampling of fluid ejections operated by inertial particles. The model proposed here and derived in the limit of negligible particle inertia is able to explain both these phenomena, from a quantitative point of view for $St^+ \leqslant 1$ and qualitatively for larger St^+. In this study, we limit the analysis to the case of dilute suspensions (one-way coupling regime); at higher particle concentrations, inter-particle interactions and collisions are expected to further reduce the wall concentration both in Newtonian and Non-Newtonian cases (see Vance *et al.* 2006).

We remark that the decrease of the wall-normal fluid velocity fluctuation is a signature of drag reduction in turbulent flows, so we expect that a reduced turbophoresis is a common feature of all turbulent flows of reduced drag and not only of polymeric flows. The reduced wall accumulation can be exploited in all applications where an increase of the bulk transport of the particle phase is needed. Turbophoresis reduces the mass flux of the particulate phase since particles tend to concentrate at the wall where the mean streamwise fluid velocity is vanishing. The reduced amount of turbophoresis combined with the increase of the fluid flow rate caused by the drag reduction is expected to substantially increase the particle mass flux.

The present study provides a more general understanding of the mechanisms of turbophoresis and their relation to the turbulence characteristics, in particular the wall-normal variations of wall-normal velocity fluctuations near the wall. An alteration of the Reynolds stress intensities is also found in other turbulent wall flows, e.g. in presence of wall roughness, where the model we adopt can be fruitfully exploited to understand and estimate the turbophoresis modification.

REFERENCES

BEC, J., BIFERALE, L., CENCINI, M., LANOTTE, A., MUSACCHIO, S. & TOSCHI, F. 2007 Heavy particle concentration in turbulence at dissipative and inertial scales. *Physical Review Letters* **98** (8), 84502.

CAPORALONI, M., TAMPIERI, F., TROMBETTI, F. & VITTORI, O. 1975 Transfer of particles in nonisotropic air turbulence. *Journal of Atmospheric Sciences* **32**, 565–568.

CHEVALIER, M., SCHLATTER, P., LUNDBLADH, A. & HENNINGSON, D. S. 2007 Simson: A pseudo-spectral solver for incompressible boundary layer flows. *Tech. Rep.* TRITA-MEK 2007:07. KTH Mechanics.

CHHABRA, RP, UHLHERR, PHT & BOGER, DV 1980 The influence of fluid elasticity on the drag coefficient for creeping flow around a sphere. *Journal of Non-Newtonian Fluid Mechanics* **6** (3), 187–199.

DE ANGELIS, E., CASCIOLA, C.M., L'VOV, V.S., POMYALOV, A., PROCACCIA, I. & TIBERKEVICH, V. 2004 Drag reduction by a linear viscosity profile. *Physical Review E* **70** (5), 055301.

DE ANGELIS, E., CASCIOLA, C.M. & PIVA, R. 2002 Dns of wall turbulence: dilute polymers and self-sustaining mechanisms. *Computers & fluids* **31** (4), 495–507.

DE LILLO, F., BOFFETTA, G. & MUSACCHIO, S. 2012 Control of particle clustering in turbulence by polymer additives. *Physical Review E* **85** (3), 036308.

GRINDLE, T.J., BURCHAM, F.W. & HUGH, L. 2003 *Engine damage to a NASA DC-8-72 airplane from a high-altitude encounter with a diffuse volcanic ash cloud.* NASA/TM-2003-212030.

LEE, P.F.W. & DUFFY, G.G. 1976 Relationships between velocity profiles and drag reduction in turbulent fiber suspension flow. *AIChE Journal* **22** (4), 750–753.

LIU, B.Y.H. & AGARWAL, J.K. 1974 Experimental observation of aerosol deposition in turbulent flow. *Journal of Aerosol Science* **5** (2), 145–155.

MARCHIOLI, C., SOLDATI, A., KUERTEN, J.G.M., ARCEN, B., TANIERE, A., GOLDENSOPH, G., SQUIRES, K.D., CARGNELUTTI, M.F. & PORTELA, L.M. 2008 Statistics of particle dispersion in direct numerical simulations of wall-bounded turbulence: Results of an international collaborative benchmark test. *International Journal of Multiphase Flow* **34** (9), 879–893.

MAXEY, M.R. & RILEY, J.J. 1983 Equation of motion for a small rigid sphere in a nonuniform flow. *Physics of Fluids* **26**, 883.

PICANO, F., BATTISTA, F., TROIANI, G. & CASCIOLA, C.M. 2011 Dynamics of piv seeding particles in turbulent premixed flames. *Experiments in Fluids* **50** (1), 75–88.

PICANO, F., SARDINA, G. & CASCIOLA, C.M. 2009 Spatial development of particle-laden turbulent pipe flow. *Physics of Fluids* **21**, 093305.

REEKS, M.W. 1983 The transport of discrete particles in inhomogeneous turbulence. *Journal of aerosol science* **14** (6), 729–739.

ROUSON, D.W.I. & EATON, J.K. 2001 On the preferential concentration of solid particles in turbulent channel flow. *Journal of Fluid Mechanics* **428** (1), 149–169.

SARDINA, G., SCHLATTER, P., BRANDT, L., PICANO, F. & CASCIOLA, C.M. 2012*a* Wall accumulation and spatial localization in particle-laden wall flows. *Journal of Fluid Mechanics* **699** (1), 50–78.

SARDINA, G., SCHLATTER, P., PICANO, F., CASCIOLA, C.M., BRANDT, L. & HENNINGSON, D.S. 2012*b* Self-similar transport of inertial particles in a turbulent boundary layer. *Journal of Fluid Mechanics* **706** (1), 584–596.

SELLIN, R.H.J., HOYT, J.W. & SCRIVENER, O. 1982 The effect of drag-reducing additives on fluid flows and their industrial applications part 1: basic aspects. *Journal of Hydraulic Research* **20** (1), 29–68.

SOLDATI, A. & MARCHIOLI, C. 2009 Physics and modelling of turbulent particle deposition and entrainment: Review of a systematic study. *International Journal of Multiphase Flow* **35** (9), 827–839.

SURESHKUMAR, R., BERIS, A.N. & HANDLER, R.A. 1997 Direct numerical simulation of the turbulent channel flow of a polymer solution. *Physics of Fluids* **9** (3), 743–755.

TSINOBER, A. 1990 Mhd flow drag reduction. *Viscous drag reduction in boundary layers* **123**, 327–349.

URBAN, DIETER & TAKAMURA, KOICHI 2002 *Polymer dispersions and their industrial applications*. Wiley-VCH Verlag GmbH & Co. KGaA.

VAN DEN BERG, T.H., LUTHER, S., LATHROP, D.P. & LOHSE, D. 2005 Drag reduction in bubbly taylor-couette turbulence. *Physical review letters* **94** (4), 44501.

VANCE, MARION W, SQUIRES, KYLE D & SIMONIN, OLIVIER 2006 Properties of the particle velocity field in gas-solid turbulent channel flow. *Physics of Fluids* **18**, 063302.

VIRK, P.S. 1975 Drag reduction fundamentals. *American Institute of Chemical Engineers, Journ of* **21** (4).

VISCONTI, I CRIVELLI, LANGELLA, A & DURANTE, M 2001 The wear behaviour of composite materials with epoxy matrix filled with hard powder. *Applied Composite Materials* **8** (3), 179–189.

VOGLER, TJ, ALEXANDER, CS, WISE, JL & MONTGOMERY, ST 2010 Dynamic behavior of tungsten carbide and alumina filled epoxy composites. *Journal of Applied Physics* **107** (4), 043520–043520.

WANG, L.P. & MAXEY, M.R. 1993 Settling velocity and concentrations distribution of heavy particles in homogeneous isotropic turbulence. *Journal of Fluid Mechanics* **256**, 27–68.

WU, Z. & YOUNG, J.B. 2012 The deposition of small particles from a turbulent air flow in a curved duct. *International Journal of Multiphase Flow* .

XI, L. & GRAHAM, M.D. 2010 Active and hibernating turbulence in minimal channel flow of newtonian and polymeric fluids. *Physical Review Letters* **104** (21), 218301.

YOUNG, J. & LEEMING, A. 1997 A theory of particle deposition in turbulent pipe flow. *Journal of Fluid Mechanics* **340** (1), 129–159.

Zaichik, L.I. 1999 A statistical model of particle transport and heat transfer in turbulent shear flows. *Physics of Fluids* **11**, 1521.